Enhanced mechanical properties in ultrafine grained 7075 Al alloy

Y.H. Zhao, X.Z. Liao, and Y.T. Zhu[a)]
Materials Science and Technology Division, Los Alamos National Laboratory, Los Alamos, New Mexico 87545

R.Z. Valiev
Institute of Physics of Advanced Materials, Ufa State Aviation Technical University, 450000 Ufa, Russian Federation

(Received 22 May 2004; accepted 4 November 2004)

Highest strength for 7075 Al alloy was obtained by combining the equal-channel-angular pressing (ECAP) and natural aging processes. The tensile yield strength and ultimate strength of the ECAP processed and naturally aged sample were 103% and 35% higher, respectively, than those of the coarse-grained 7075 Al alloy counterpart. The enhanced strength resulted from high densities of Guinier–Preston (G-P) zones and dislocations. This study shows that severe plastic deformation has the potential to significantly enhance the mechanical properties of precipitate hardening 7000 series Al alloys.

Precipitate strengthening 7000 series Al alloys possess the highest strength among all commercial Al alloys and are widely used for structural applications in military and civil aircraft as well as sporting goods. The 7000 Al alloys are strengthened by a high density of Guinier–Preston (G-P) zones because the strong atomic bonds in the zones can increase the resistance to dislocation movement.[1,2] For the Al–Zn–Mg–Cu 7075 system, a high density of G-P zones can be achieved by aging at low temperature (such as room temperature) after solution treatment.[3,4] Cold work, which usually improves the strength of metals and alloys, has been found to be ineffective in improving the strength of 7000 series Al alloys. This was explained by the viewpoint that dislocation did not greatly accelerate the G-P zone precipitation.[5] In the last decade, cqual-channel-angular pressing (ECAP)[6] has been found to enhance mechanical strength significantly by introducing ultrafine grained (UFG) structures into bulk materials. It is of great interest to investigate whether the strengthening effect of the ECAP process can be added to the precipitate strengthening in 7000 series Al alloys. If these two strengthening effects can be made additive, it will be possible to significantly improve the strength of 7000 Al alloys, making them much more attractive in high-strength structural applications.

In this work, 7075 Al alloy was selected and processed by combining ECAP and natural aging processes. The results demonstrate that ECAP process can add significant strengthening effect to the precipitate strengthening in 7075 Al alloy. The two strengthening effects were understood from microstructural characteristic of the UFG 7075 Al alloy (G-P zone, grain size, dislocation density and lattice parameter).

Commercial 7075 Al alloy, homogenized by solution treatment (at 480 °C for 5 h) and quenched to room temperature, was used immediately for the ECAP process. The sample was pressed through a die for 2 passes with an intersecting channel angle of 90° and an outerarc angle 45° by route B_c. In the B_c route, the work piece was rotated 90° along its longitudinal axis between two adjacent passes.[7] The present die configuration imposes an equivalent strain (von Mises strain) of approximately one per ECAP pass.[8] The ECAP-processed UFG and initially homogenized coarse-grained (CG) samples were then naturally aged at room temperature for one month.

Tensile tests were carried out using a Shimadzu Universal Tester (Kyoto, Japan). The samples were cut and polished into a 2.0 × 1.4 mm cross section and a gauge length of 18.0 mm for tensile tests. Five specimens were used to obtain a consistent stress–strain curve for the UFG and CG samples. All the specimens were tested at a displacement rate of 1×10^{-2} mm/s and with the tensile direction parallel to the longitudinal axis. X-ray diffraction (XRD) measurements were performed on a Scintag x-ray diffractometer (Cupertino, CA) operating at 1.8 kW, and equipped with a Cu target and a secondary monochromator to select the Cu K_α radiation. θ-2θ accurate scans with a step size of $2\theta = 0.02°$ and a counting time of 10 s were performed at room temperature. Pure Al powder (99.999%)

a)Address all correspondence to this author.
e-mail: yzhu@lanl.gov
DOI: 10.1557/JMR.2005.0057

was annealed at 200 °C in Ar and used as a XRD reference. Transmission electron microscopy (TEM) and high-resolution TEM (HREM) were performed on a Phillips CM30 (Potomac, MD) microscope operating at 300 kV and a JEOL 3000F (Tokyo, Japan) microscope operating at 300 kV, respectively. The TEM and HREM specimens were prepared by mechanical grinding each side of the sample to about 10 μm thick using diamond lapping films (with particle diameters of 30, 6, 1, 0.1 μm in order). Further thinning to a thickness of electron transparency was carried out using a Gatan Dual Ion Milling System (Pleasanton, CA) with an Ar^+ accelerating voltage of 4 kV and liquid nitrogen for cooling the specimen. The above TEM specimen preparation did not change the structure of the initially processed samples.

The typical engineering stress-strain curves of the UFG and CG samples are shown in Fig. 1. The naturally aged UFG sample has a much higher strength than the CG sample. The tensile yield strength and ultimate strength of the UFG sample are 650 and 720 MPa, respectively, which are about 103% and 35% higher than those of the CG sample (320 and 530 MPa). The elongation to failure of the UFG sample (8.39%) is smaller than that of the CG sample (20. 51%). To authors' knowledge, the present strength of the UFG 7075 Al alloy is the highest value of 7075 Al alloy in literature.[5]

To discover the strengthening reasons of the UFG sample, TEM, HREM, and XRD were used to analyze the microstructure. Figure 2(a) shows the TEM picture of the UFG sample. The UFG sample was composed of lamella grains with an average length of about 430 nm and a width of about 150 nm. The grain boundaries of the UFG sample are wavy and diffuse, corresponding to high-energy non-equilibrium boundary configuration.[9,10] Moreover, there are many fringes and networks within the grains. One-dimensional HREM image (obtained by Fourier and inverse Fourier transformations of the original HREM image) indicates that these fringes and

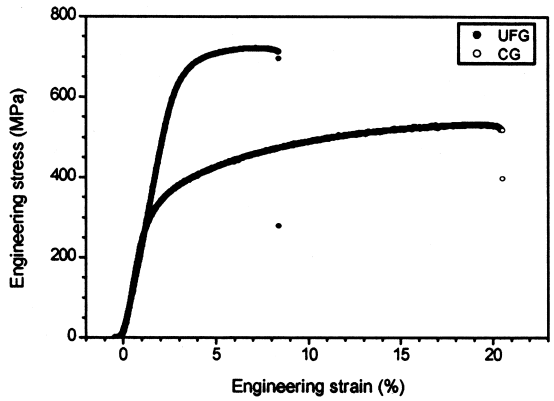

FIG. 1. Tensile engineering stress-strain curves for the (●) UFG and (○) CG samples, both of which were naturally aged for one month. Five specimens were used to obtain a consistent stress-strain curve for the UFG and CG samples.

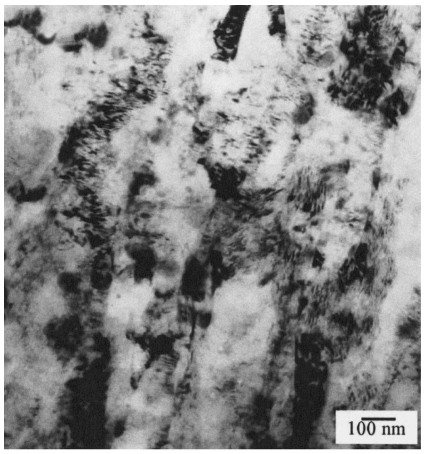

(a)

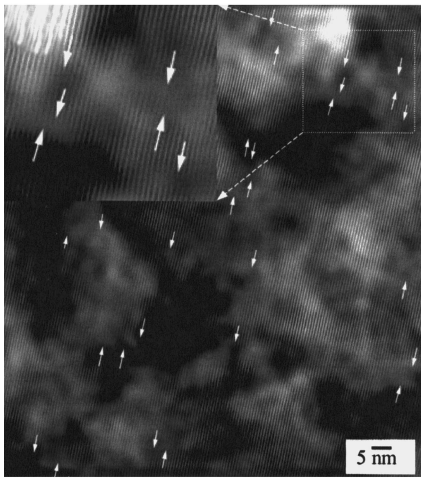

(b)

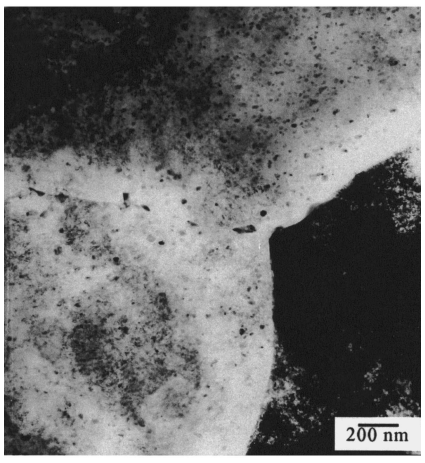

(c)

FIG. 2. TEM and HREM pictures of the (a, b) UFG and (c) CG samples; (b) is one-dimensional HREM image obtained by Fourier and inverse Fourier transformations of the original HREM image. The end of each half atomic plane, which is the core position of a dislocation line, is marked with white arrows. The inset is the magnified figure of the square area marked in (b).

networks are corresponding to a high density of dislocations, as shown in Fig. 2(b). The white arrow in Fig. 2(b) marks the end of each half atomic plane, which is the core position of a dislocation line. The CG sample has equiaxed grains with a size of about 42 μm. The grain boundaries are straight and sharp, and the dislocation density is very low, as shown in Fig. 2(c).

The average grain size and microstrain can be calculated using XRD peak broadening method,[11] as listed in Table I. The XRD calculated average grain size of the UFG sample is about 70 ± 15 nm, which is much smaller than the TEM result (290 ± 20 nm). This is because XRD measures the coherent diffraction domain size, which is subgrain/dislocation cell size.[12,13] The average microstrain of the UFG sample is 0.54 ± 0.04%, which is significantly larger than that of the CG sample (0.05 ± 0.02%). According to the grain size and microstrain, one can estimate dislocation density in the UFG and CG samples.[14,15] As listed in Table I, the average dislocation density of the UFG sample is 0.94×10^{15} m^{-2}, which is significantly larger than that in the CG sample (0.002×10^{15} m^{-2}). The dislocation densities averaged from numerous HREM observations in different areas were 0.96×10^{15} m^{-2} for the UFG sample and 0.001×10^{15} m^{-2} for the CG sample, agreeing with the XRD results, as listed in Table I. The lattice parameter of the UFG and CG 7075 Al alloys, calculated from the XRD peak positions, are nearly the same, equal to 4.056 ± 0.001 Å.

From Fig. 2, besides the structural imperfections, there precipitated the second phases in the UFG and CG samples. Figure 3 shows the XRD patterns of the UFG and CG samples. Besides the Bragg reflections from the Al matrix, there appeared a broad peak at about $2\theta = 20°$ and some other weak peaks. The broad peak responds to the G-P zones, which was verified in Ref. 16, and the other weak peaks are from the metastable hexagonal η′ phase, whose reflection indexes were indicated in the figure. Because the XRD samples have the same areas

TABLE I. A list of the yield strengths (σ_{ys}), ultimate strengths (σ_{us}), elongation to failure (ϵ_{ef}), grain sizes (D), microstrains ($\langle\epsilon^2\rangle^{1/2}$), dislocation densities (ρ) and lattice parameters (a) of the UFG and CG 7075 Al alloys. The errors of the XRD calculated grain size and microstrain are about 15 nm and 0.04% respectively, and the error of the lattice parameter is about 0.001 Å.

Samples		UFG 7075 Al alloy	CG 7075 Al alloy
σ_{ys} (MPa)		650	320
σ_{us} (MPa)		720	530
ϵ_{ef} (%)		8.39	20.51
…	XRD	70	…
D (nm)	TEM	290	42,000
$\langle\epsilon^2\rangle^{1/2}$ (%)		0.54	0.05
…	XRD	0.94	0.002
ρ (10^{15} m^{-2})	HREM	0.96	0.001
a (Å)		4.056	4.056

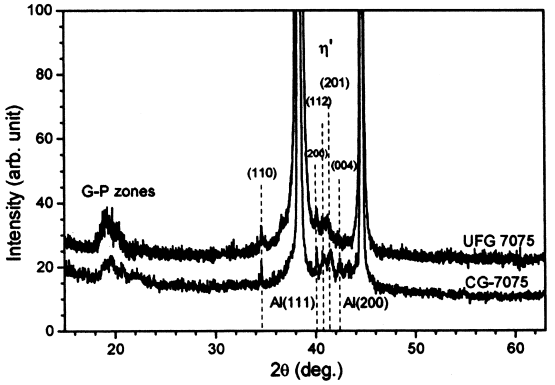

FIG. 3. XRD patterns of the UFG and CG samples. The broad peak at about 20° corresponds to the G-P zones, and the reflection indexes of η′ phase are indicated.

involved in the reflection, the intensity of the XRD patterns can be compared. From Fig. 3, the intensity of the G-P zone broad peak of the UFG sample is larger than that of the CG sample, indicating that the volume fraction of the G-P zones in the UFG sample is larger than that in the CG sample. The peak intensity of the η′ phase in the CG sample is a little larger than that in the UFG sample, meaning that the volume fraction of the η′ phase in the CG sample is larger than that in the UFG sample.

The above phase precipitation can be observed by HREM, as shown in Figs. 4(a) and 4(b). Both the coherent spherical G-P zones [as shown by the arrows in Fig. 4(a)] and semi-coherent plate-shaped η′ phase [see Fig. 4(b)] are observed in the UFG and CG samples. The density of the G-P zones in the UFG sample is larger than that in the CG sample, agreeing with the XRD results.

Our experiments indicate that the ECAP processed and naturally aged 7075 Al alloy possesses much higher strength compared with the CG counterpart. Such enhanced strength may be attributed to (i) solid solution strengthening, (ii) grain refinement strengthening, (iii) dislocation strengthening, and (iv) precipitation

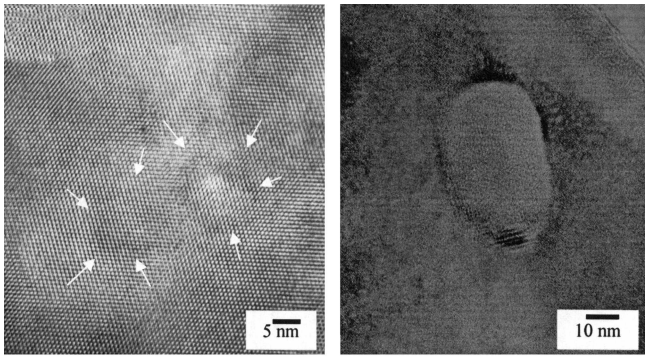

FIG. 4. HREM images of the (a) UFG and (b) CG samples observed from the [110] direction of the Al matrix. The arrows in (a) indicate the spherical coherent G-P zones; (b) represents the semi-coherent plate-shaped η′ phase.

strengthening. The solid solution strengthening can be excluded because of the same lattice parameters (solid solubility) of the UFG and CG Al matrix. In Ref. 16, we verified that the grain refinement strengthening was not the main contributor for the enhanced strength of the UFG sample. So, the enhanced strength of the UFG sample mainly results from the G-P zone and dislocation strengthening. The dislocation networks and tangles within grains and near grain or subgrain boundaries make dislocation glide more difficult. The strong atomic bonds in the G-P zones and higher density of the G-P zones can effectively increase the resistance foe dislocation cutting through the zones. Both XRD and HREM revealed that the densities of the G-P zones and dislocations in the UFG sample are larger than that in the CG sample. Therefore, the cooperative interaction of the high densities of the G-P zones and dislocations has resulted in the significantly enhanced strength of the UFG 7075 Al alloy.

In the literature,[17,18] for 7075 Al alloys, the processes of room-temperature rolling (the reduction in thickness less than 50%) and aging (105–150 °C) after solution treatment did not increase the hardness compared with the aged sample. While the present result shows that the ECAP process and natural aging after solution treatment can increase the strength greatly. This difference is caused by (i) the different aging temperatures and (ii) different deformation strains. In the literature,[17,18] the aging temperature is between 105 and 150 °C. Our most recent study shows these temperatures can cause the defects (dislocations) recovery[19,20] and overcompensate the aging hardening. The natural aging keeps the defect strengthening effect, and the combination of aging hardening and work hardening result in the observed enhanced strength. The present strain (2, equal to 82% thickness reduction by rolling) imposed by ECAP is larger than that induced by room-temperature rolling (<50%).

The larger volume fraction of the G-P zones in the UFG sample than that in the CG sample indicates that the ECAP process accelerates the precipitation of the G-P zones. HREM studies did not observe dislocations within most of the G-P zones in the UFG sample. For the other small amount of the G-P zones, there are dislocations at the edge of the G-P zones. This suggests that the large amount of the G-P zones precipitated in the UFG sample were not driven by dislocation. In the literature,[4] it was reported that the nucleation of the G-P zones were mainly controlled by the concentration of vacant lattice sites. Further studies on the concentration of vacancy are in progress.

In brief, a combination of ECAP processing and precipitate strengthening has the potential to render 7000 series Al alloys significantly stronger than those processed by either technique alone. The high densities of G-P zones and dislocations are primarily responsible for the high strength of the UFG 7075 Al alloy.

REFERENCES

1. W.F. Smith and N.J. Grant: The effect of multi-step aging on the strength properties and precipitate-free zone widths in Al-Zn-Mg alloys. *Metall. Trans.* **1,** 979 (1970).
2. A. Kelly and R.B. Nicholson: Precipitate hardening. *Prog. Mater. Sci.* **10,** 216 (1963).
3. G. Thomas and J. Nutting: The aging characteristics of aluminum alloys. *J. Inst. Met.* **88,** 81 (1959).
4. J.D. Embury and R.B. Nicholson: The nucleation of precipitates: The system Al-Zn-Mg. *Acta Metall.* **13,** 403 (1965).
5. W.F. Smith: *Structure and Properties of Engineering Alloys* (McGraw-Hill, New York, 1993), Chap. 5–9, pp. 209–215.
6. R.Z. Valiev, R.K. Islamgaliev, and I.V. Alexandrov: Bulk nanostructured materials from severe plastic deformation. *Prog. Mater. Sci.* **45,** 103 (2000).
7. Y.T. Zhu and T.C. Lowe: Observations and issues on mechanisms of grain refinement during ECAP process. *Mater. Sci. Eng.* **A291,** 46 (2000).
8. Y. Iwahashi, J. Wang, Z. Horita, M. Memoto, and T.G. Langdon: Principle of equal-channel angular pressing for the processing of ultra-fine grained materials. *Scripta Mater.* **35,** 143 (1996).
9. D.G. Morris and M.A. Munoz-Morris: Microstructure of severely deformed Al-3Mg and its evolution during annealing. *Acta Mater.* **50,** 4047 (2002).
10. J. Wang, Y. Iwahashi, Z. Horita, M. Furukawa, M. Nemoto, R.Z. Valiev, and T.G. Langdon: An investigation of microstructural stability in an Al-Mg alloy with submicrometer grain size. *Acta Mater.* **44,** 2973 (1996).
11. Y.H. Zhao, K. Zhang, and K. Lu: Structure characteristics of nanocrystalline element selenium with different grain sizes. *Phys. Rev. B.* **56,** 14322 (1997).
12. T. Ungar: The meaning of size obtained from broadened x-ray diffraction peaks. *Adv. Eng. Mater.* **5,** 323 (2003).
13. J. Gubicza, I.C. Dragomir, G. Ribarik, Y.T. Zhu, R.Z. Valiev, and T. Ungar: Characterization of the microstructures of severely deformed titanium by x-ray diffraction profile analysis. *Mater. Sci. Forum.* **229,** 414 (2003).
14. Y.H. Zhao, H.W. Sheng, and K. Lu: Microstructure evolution and thermal properties in nanocrystalline Fe during mechanical attrition. *Acta Mater.* **49,** 365 (2001).
15. Y.H. Zhao, K. Zhang, and K. Lu: Microstructure evolution and thermal properties in nanocrystalline Cu during mechanical attrition. *Phys. Rev. B.* **66,** 085404 (2002).
16. Y.H. Zhao, X.Z. Liao, J. Jin, R.Z. Valiev, and Y.T. Zhu: In *Ultrafine-Grained Materials III,* edited by Y.T. Zhu, T.G. Langdon, R.Z. Valiev, S.L. Semiatin, D.H. Sin, and T.C. Lowe (TMS, Warrendale, PA, 2004), p. 511.
17. E. Di Risso, M. Conserva, F. Gatto, and H. Markus: Thermomechanical treatments on high strength Al-Zn-Mg(-Cu) alloys. *Metall. Trans.* **4,** 1133 (1973).
18. M. Consera, M. Nuratti, E. Di Risso, and F. Gatto: Age hardening behavior of TMT processed Al-Zn-Mg-Cu alloy. *Mater. Sci. Eng.* **11,** 103 (1973).
19. Y.H. Zhao, X.Z. Liao, R.Z. Valiev, and Y.T. Zhu: Structures and mechanical properties of ECAP processed 7075 Al alloy upon natural aging and T651 treatment, in *Nanoscale Materials and Modeling—Relations Among Processing Microstructure and Mechanical Properties,* edited by P.M. Anderson, T. Foecke, A. Misra, and R.E. Rudd. (Mater. Res. Soc. Symp. Proc. **821,** Warrendale, PA, 2004), p. 59.
20. Y.H. Zhao, X.Z. Liao, Z. Jin, R.Z. Valiev, and Y.T. Zhu: Microstructures and mechanical properties of ultrafine grained 7075 Al alloy processed by ECAP and their evolutions during annealing. *Acta Mater.* **52,** 4589 (2004).